A mechanistic investigation of the coupled reaction of n-hexane and methanol over HZSM-5

Fuxiang Chang [a,b], Yingxu Wei [a], Xianbin Liu [a,b], Yinfeng Zhao [a,b], Lei Xu [a],
Ying Sun [a,b], Dazhi Zhang [a,b], Yanli He [a], Zhongmin Liu [a,*]

[a] Natural Gas Utilization and Applied Catalysis Laboratory, Dalian Institute of Chemical Physics, Chinese Academy of Sciences,
P.O. Box 110, 116023 Dalian, PR China
[b] Graduate School of the Chinese Academy of Sciences, Beijing 100039, PR China

Abstract

The coupled reaction of n-hexane and methanol was studied and compared with the reactions of individual reactants over HZSM-5 zeolite catalyst. The catalytic reaction test results and the temperature-programmed surface reaction (TPSR) results showed an improvement of the initial n-hexane activity when methanol was used as co-reactant. The FT-IR analysis indicated that methanol was adsorbed on acid sites prior to n-hexane and immediately transformed into surface methoxy groups. These species acted as the active sites for the conversion of n-hexane and improved the initial activity of n-hexane by bimolecular hydride transfer. The catalytic test also suggested that alkenes resulting from the transformation of methanol further enhance the conversion of n-hexane, in addition to the improvement by methoxy groups. A faster conversion of methanol was also observed in the coupled system, which highlights a bidirectional promotion effect of the coupled reaction. A reaction mechanism is proposed to explain all observations.

© 2007 Elsevier B.V. All rights reserved.

Keywords: Coupled reaction; n-Hexane; Methanol; ZSM-5; Mechanism

1. Introduction

Light olefins, such as ethene, propene, and butenes, are important intermediates of polymers and various petrochemicals. Such olefins are mostly produced by steam cracking of naphtha and light alkane feedstocks at high temperatures even up to 800 °C. These processes are highly energy consuming and less effective due to their thermal cracking character. Catalytic cracking of naphtha [1,2] and catalytic transformation of methanol [3,4] that could be obtained from C1 resources such as coal and natural gas rather than oil have both been studied for the development of alternative processes of light olefin production. The two reactions are evidently different considering the change of chain-length of the reactants and products, the possible reaction mechanisms and the reaction heat effects. However, the two reactions are both catalyzed by

acid zeolite catalyst, so they could be combined together in principle due to their very similar acid-catalyzing character. In view of the energy balance and the yield enhancement of target products, the effective coupling of endothermic hydrocarbon cracking with exothermic methanol conversion, first proposed by Nowak et al. [5], should be a promising reaction. Some work has been performed in this field of coupled conversion of methanol and hydrocarbon, focused on reaction condition and zeolite catalysts for higher light olefin yields. Lücke and Martin [6] thus studied the coupled transformation of methanol with C_4 hydrocarbon, liquid hydrocarbon and crude naphtha participation between 600 and 700 °C. Gao et al. [7] investigated the coupled conversion of methanol and C_4 hydrocarbons over Ga/HZSM-5 catalyst at moderate temperatures (<550 °C). Erofeev et al. [8] also worked in this field of methanol-coupled conversion of propane and butane on MFI zeolite; they emphasized the modification effect of alkaline-earth metals in the formation of light olefins. Little has been done to probe into the mechanisms of such coupled reactions. The difficulty of investigating the reaction mechanism is that the conversions of

the two reactants are quite different [9–13], leading to some complexity of the coupled system. For *n*-hexane cracking over zeolite catalysts, two mechanisms have been suggested: monomolecular and bimolecular [11–20]. In the monomolecular cracking mechanism, the initial reaction involves the formation and further decomposition of a penta-coordinated carbonium ion, with the formation of methane, hydrogen, ethane and ethene as characteristic products. The bimolecular cracking mechanism is a classical chain process involving hydride transfer between an alkane molecule and a surface carbenium ion, followed by isomerization, alkylation and β-scission of the carbenium ion. The presence of alkenes in the reaction system would greatly affect the alkane cracking due to the quick formation of more carbenium ions [20–23]. For the catalytic conversion of methanol to hydrocarbons on acid molecular sieve catalysts, some investigations suggested that the reaction is dominated by a ''hydrocarbon pool'' mechanism [24–27]. The detailed mechanism of first C–C bond formation is still unclear in methanol conversion reactions; however, many experimental studies and theoretical calculations [28–36] support the conclusion that the first C–C bond is closely correlated with the existence of surface methoxy groups. Such a correlation suggests that surface methoxy groups are very likely the most important active species.

We previously investigated the coupled reaction of *n*-hexane and methanol over HZSM-5 zeolites [37], and found an improvement of *n*-hexane activity and an increased contribution of the faster bimolecular mechanism to the *n*-hexane conversion by methanol. However, the intermediate species and the detailed mechanism for the coupled system are still unknown. To further understand the coupled system, we tested in this work the methanol coupled *n*-hexane cracking and we compared our results with the individual results of *n*-hexane reactions and methanol reactions. TPSR (temperature-programmed surface reactions) and FT-IR techniques were applied to determine the conversion improvement caused by methanol and the detailed reaction route of the coupled system was discussed.

2. Experimental

2.1. Catalyst and catalytic testing

The catalyst preparation and the catalytic test procedure have been described previously [37]. HZSM-5 (Si/Al = 19, BET surface area = 363 m^2/g) zeolite (obtained from NanKai University) was employed in this work. The experiments were carried out on a pulse reaction system based on a VARIAN CP-3800 gas chromatograph (GC) containing a 6-way valve connecting with the reactant stream and a 10-way valve connecting with the reactor inlet stream. A reactant mixture stream of *n*-hexane (90%) and methanol (10%), generated by saturating the carrier gas (He), continuously passed through the 6-way valve. The reactant stream could be injected into the reactor by the 10-way valve at atmospheric pressure. After eluting the reactor, the product stream was sent to the GC equipped with a capillary column (PONA, 100 m × 0.25 mm) and a FID detector for product analysis. The conversion of the

reactants and the yield of reaction products were expressed on a molar carbon atom basis, as described elsewhere [37].

2.2. FT-IR studies

2.2.1. Co-adsorption of methanol and n-hexane with continuous flow mode

In situ FT-IR spectra were measured on a Bruker EQUINOX 55 single-beam Fourier transform infrared spectrometer. All spectra were recorded with 16 scans with a resolution of 4 cm^{-1}. The HZSM-5 zeolite sample wafer was mounted in a high temperature/high pressure cell fitted with ZnSe windows. The sample was activated in He flow at 450 °C for 3 h. After activation, reference spectra of the fresh disk were recorded in flowing He at various temperatures. Subsequently, the reactant mixture gas flow (He:C$_6$H$_{14}$:CH$_3$OH = 50:2:1) was introduced to the cell and the spectra were recorded between 200 and 400 °C. In each case, the difference spectra were obtained by subtracting the spectra of fresh zeolite from the spectra recorded for the reactant mixture at the same temperature. When He/*n*-hexane or He/methanol as reactant flow, the difference spectra at various temperatures were recorded in the same way.

2.2.2. Adsorption of methanol at different temperatures

FT-IR spectra of methanol adsorption on HZSM-5 zeolite at different temperatures were recorded on a Bruker EQUINOX 55 FT-IR spectrometer. The HZSM-5 zeolite sample wafer was activated at 400 °C for 4 h in a quartz cell under vacuum. Then methanol vapor was introduced into the IR cell to contact zeolite wafers for 10 min at a certain temperature for adsorption. The IR cell was further evacuated for 20 min at the same temperature to remove extra methanol in the cell. The spectra were recorded at different temperatures. Difference spectra were obtained by subtracting the spectra before and after adsorption at the same temperature.

2.3. Temperature-programmed surface reaction (TPSR)

TPSR experiments were carried out in a quartz reactor (3 mm i.d.). Prior to the experiment, a fresh zeolite sample was pretreated in situ by heating to 550 °C for 1 h in a flow of N$_2$ and then cooled to 100 °C. The reactant stream carried by the carrier gas (He) continuously passed through the catalyst bed with a constant gas flow rate of 14 ml/min for 30 min. Then the reactor was heated from 100 to 500 °C at a heating rate of 8 °C/min. Gas products leaving the reactor were kept at 100 °C and simultaneously monitored by an on-line Omnistar mass spectrometer.

3. Results

3.1. Coupled transformations of n-hexane and methanol at 400 °C

In our previous research [37], when the coupled reaction was tested between 400 and 500 °C, we observed that the increase in
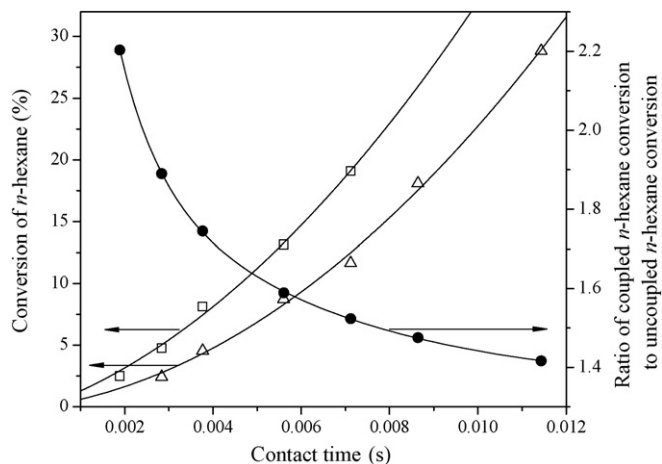
Fig. 1. Conversions of *n*-hexane without methanol coupling (△) and with methanol coupling (□) and ratio of coupled *n*-C$_6$ conversion and uncoupled *n*-C$_6$ conversion (●) vs. contact time at 400 °C over HZSM-5 zeolite (Si/Al = 19).

time, which strongly suggests that the introduction of methanol could enhance the initial activation of *n*-hexane conversion.

The yields (C%) versus contact time of the major products, the light alkanes, are given in Figs. 2 and 3, from which the initial formation rates of alkane can be estimated from curve slopes at the zero contact time. The initial formation rates of methane and the C$_3$–C$_4$ alkanes in the coupled system are higher than those in the individual reactant systems. The initial formation rate of ethane, however, is the fastest in the reaction of *n*-hexane alone.

3.2. TPSR under "continuous-flow" condition with on-line mass analysis

3.2.1. The evolutions of n-hexane and methanol in the coupled reaction and the individual reactions

Fig. 4 gives the evolution of the signal intensity of *m/e* 57, the main ion fragment of *n*-hexane [38], from the coupled reaction and the individual reactions of *n*-hexane and methanol on HZSM-5 zeolite as a function of temperature under the "continuous-flow" conditions. In the case of methanol conversion (Fig. 4a), it is reasonable to find that the *m/e* 57 signal appears at relatively high temperature in the reactant stream, indicating the higher hydrocarbons' formation. For the individual *n*-hexane transformation (Fig. 4b), there is a sharp decrease of the *m/e* 57 signal when the temperature is higher than 168 °C and with another decrease at temperatures higher than 308 °C. For the coupled reaction of *n*-hexane and methanol (Fig. 4c), the change of *m/e* 57 with temperature is different from the case of *n*-hexane conversion, with an apparent decrease of the signal starting from 220 °C, indicating that the reaction takes place at this temperature. Comparison with the
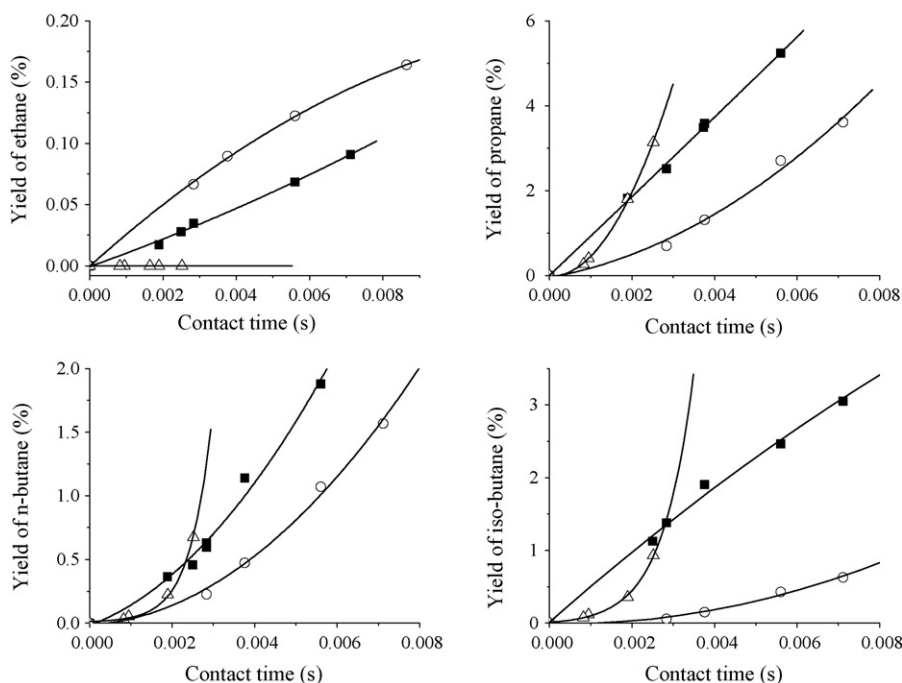
conversion rate of *n*-hexane is more pronounced at low temperature compared with the uncoupled *n*-hexane cracking. We focus on lower temperature reactions and characterization in the present work. The coupled transformations of *n*-hexane and methanol, as well as the reactions of the individual reactants, were performed over HZSM-5 catalyst at 400 °C at different contact times. The *n*-hexane conversion (C%) is evidently higher in the coupled reaction system than in the reaction of *n*-hexane alone (Fig. 1) over a large range of contact times 0.00189–0.01143 s. The relative increase of *n*-hexane conversion (the ratio of coupled *n*-C$_6$ conversion to uncoupled *n*-C$_6$ conversion) became larger with the decrease of contact

Fig. 2. Yields of C$_2$–C$_4$ alkanes vs. contact time for *n*-hexane conversion with methanol coupling (■), without methanol coupling (○), and the conversion of methanol alone (△) at 400 °C over HZSM-5 zeolite (Si/Al = 19).
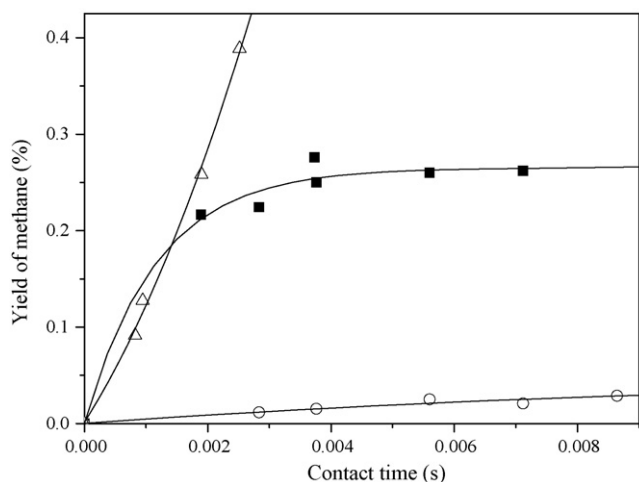
Fig. 3. Yields of methane vs. contact time for *n*-hexane conversion with methanol coupling (■), without methanol coupling (○), and the conversion of methanol alone (△) at 400 °C over HZSM-5 zeolite (Si/Al = 19).
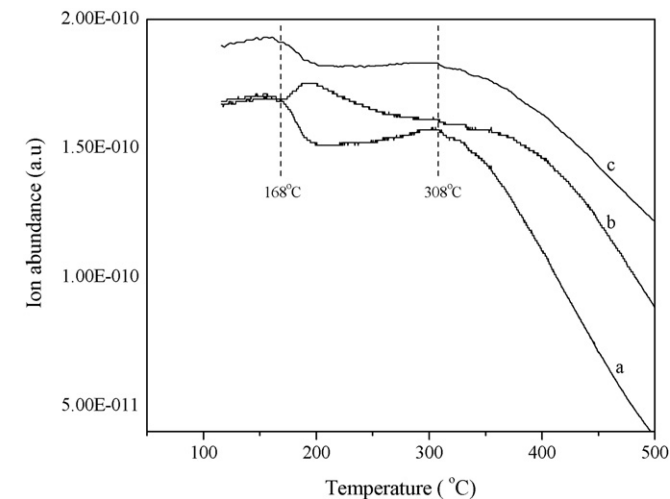

Fig. 5. Signals of different *m/e* with flow of *n*-hexane passing through H-ZSM5 zeolite as a function of temperature: (a) *m/e* = 57, (b) *m/e* = 43, and (c) *m/e* = 41.

coupled reaction, although there is indeed a decrease of *m/e* 57 observed from 168 °C, it is not easy to imagine that the *n*-hexane cracking reaction occurred at such low temperature based on our pulse catalytic reaction experience. To clarify this behavior, we also checked other ion fragments in the *n*-hexane reaction stream. Fig. 5 shows the evolution of three important mass signals of *m/e* = 41, 43 and 57, all tracking the evolution of hexane from the stream of *n*-hexane alone passing over HZSM-5 zeolite, in which the *m/e* 43 signal arises from all hexane isomers and the *m/e* 41 and 57 signals primarily arise from *n*-hexane [38]. It could be observed that both the evolution profiles of *m/e* 41 and 57 (Fig. 5) display a decrease starting from 168 °C, whereas, the evolution profile of *m/e* 43 displays a corresponding increase at the same time. This indicates that isomerization reactions of *n*-hexane occur at a low temperature of 168 °C. At higher temperatures above 308 °C, all the three evolution profiles (*m/e* 57, 43 and 41) show a gradual drop in intensity with temperature increase, suggesting that the

cracking reaction takes place at this temperature. Comparing the coupled reaction with uncoupled *n*-hexane reaction, we concluded that the starting temperature of *n*-hexane cracking reaction decreases to 220 from 308 °C due to the coupling effect of methanol and *n*-hexane reactions. In addition, it is worthy to note that only until about 352 °C are the higher hydrocarbons observed in the individual methanol reaction.

Fig. 6 gives the evolution of signals *m/e* = 18, 31, and 45 tracking the concentration of H_2O, methanol, and DME, respectively. In the case of methanol as reactant alone, it could be observed that the formation of H_2O (*m/e* = 18) and DME (*m/e* = 45) is accompanied with the decrease of methanol signal (*m/e* = 31). There is an equilibration among methanol, DME and water below 350 °C. Further increase of the temperature results in a sharp decrease of methanol and DME intensity and a second increase of water, indicating that hydrocarbon formation reaction occurs above 350 °C. In the case of coupled reactions of methanol and *n*-hexane, similar phenomena were
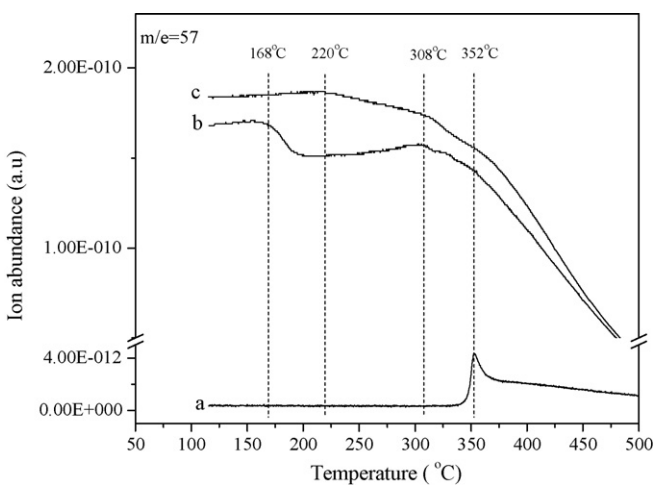

Fig. 4. Signals of *m/e* 57 with continuous flows of (a) methanol, (b) *n*-hexane, and (c) the mixture of *n*-hexane and methanol passing through H-ZSM5 zeolite as a function of temperature.
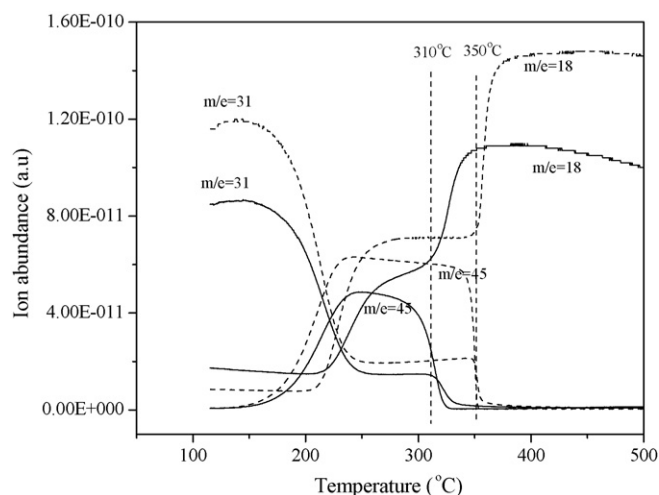

Fig. 6. Signals for the educts methanol (*m/e* = 31), the products DME (*m/e* = 45), and H_2O (*m/e* = 18) with continuous flows of (- - -) methanol and (—) of the mixture of *n*-hexane and methanol passing through H-ZSM5 zeolite as a function of temperature.
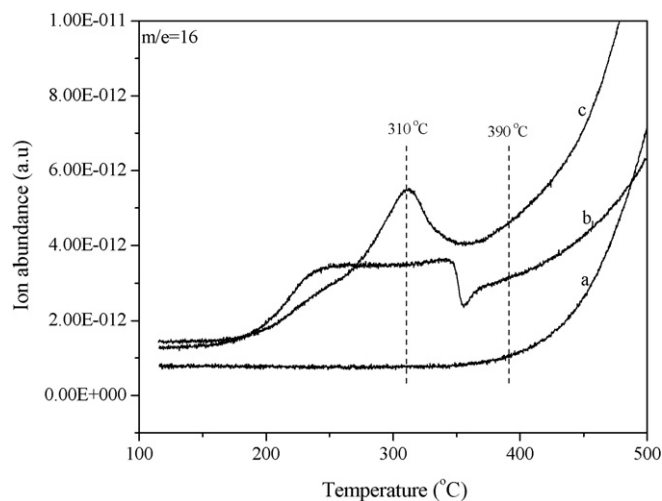
Fig. 7. The m/e 16 (methane) signals with continuous flows of (a) n-hexane, (b) methanol, and (c) the mixture of n-hexane and methanol passing through H-ZSM5 zeolite as a function of temperature.

Fig. 8. Signals of m/e 26 and m/e 2 with continuous flows of (a) n-hexane, (b) methanol, and (c) the mixture of n-hexane and methanol passing through H-ZSM5 zeolite as a function of temperature.

also observed. However, one big difference that should be noted is that the temperature of the second rapid consumption of methanol and DME is at 310 °C, a value that is 40 °C lower than in the case of methanol conversion alone. This may suggest a bidirectional promotion effect of the reactions, i.e. the coupling of the two reactions not only promotes the conversion of n-hexane, and could also enhance the conversion of methanol.

3.2.2. The evolution of other products

The mass signals of the $C_3–C_6$ hydrocarbon products could be easily detected but were overlapped greatly by the signals from the n-hexane flow [38]. In this case, the mass signals of $m/e = 2$, 16, and 26 will be more meaningful to track the evolution of corresponding products. Fig. 7 shows the evolution of methane ($m/e = 16$) under the continuous flow of n-hexane, methanol, and a mixture of both reactants. In the case of n-hexane alone (Fig. 7a), only a trace amount of methane is produced below 390 °C. Above 390 °C, the signal of methane is proportional to the temperature. This is different from methanol conversion (Fig. 7b), in which case methane has a constant value during the equilibration among methanol, DME, and water. In the case of the mixture flow, the evolution profile of methane shows a maximum at 310 °C (Fig. 7c).

Fig. 8 shows that the evolutions of $m/e = 2$ (H_2) and $m/e = 26$ (C_2 products) in the coupled system exhibit the same tendency as those in the methanol alone system at low temperature and only a lower evolution temperature is observed in co-feed conditions compared with the individual feed cases.

3.3. Conversions of n-hexane with and without methanol pre-adsorption on catalyst

The enhancement of n-hexane conversion by introducing methanol to the n-hexane reaction system may be related to the change of adsorbed surface groups and the interactions between the surface groups and n-hexane molecules. The effect of pre-adsorption of methanol on the n-hexane reaction was
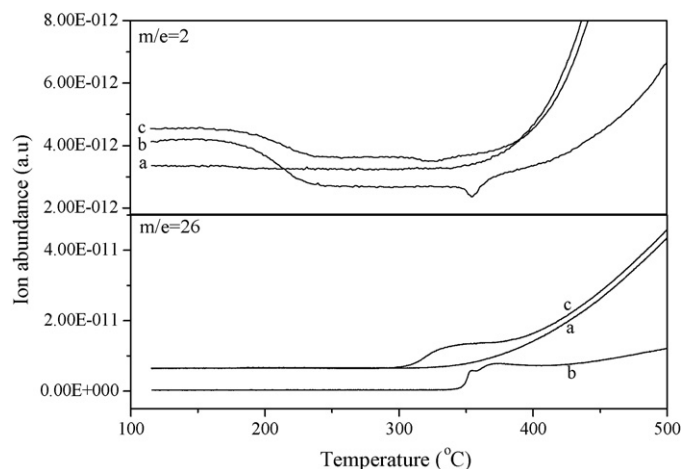
investigated between 200 and 350 °C by first contacting HZSM-5 samples with methanol stream and then performing n-hexane pulse reaction after the catalyst had been purged with nitrogen. Fig. 9 shows that there is a substantial enhancement of the n-hexane conversion after methanol pre-adsorption, especially at a lower temperature such as 250 °C.

3.4. FT-IR spectroscopic study

3.4.1. Coadsorption of n-hexane with methanol

Difference IR spectra of HZSM-5 zeolite in the v (OH) region resulting from continuously contacting of n-hexane, methanol, and their mixtures are shown and compared in Fig. 10. Under n-hexane flow (Fig. 10A), n-hexane interacts with two types of hydroxyl groups at 200 °C (Fig. 10A(a)), as seen from the negative features of the bands at 3744 and
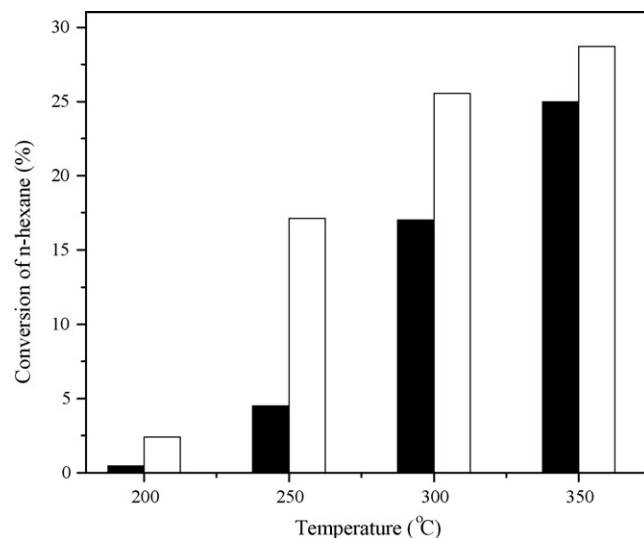

Fig. 9. The conversion of n-hexane in the temperature range of 200–350 °C on ZSM-5 zeolite catalyst with pre-adsorption methanol (□) and H-ZSM-5 zeolite catalyst (■).
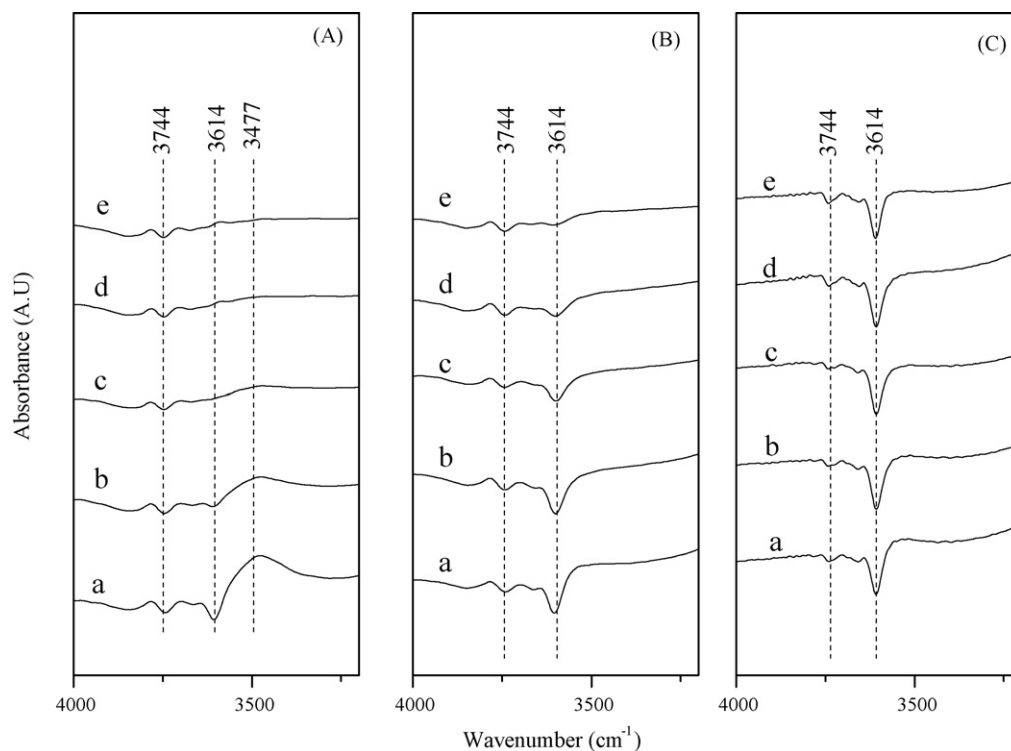
Fig. 10. Infrared difference spectra recorded on HZSM-5 zeolite with continuous flows of (A) *n*-hexane, (B) methanol, and (C) a mixture of *n*-hexane and methanol at (a) 200 °C (b) 250 °C; (c) 300 °C; (d) 350 °C; (e) 400 °C.

3614 cm^{-1}, corresponding to terminal Si(OH) and bridge hydroxyl Si(OH)Al [28–30,39,40]. A broad band centered at 3477 cm^{-1} is observed at the same time. Trombetta et al. [40] attribute the appearance of this broad band to the interaction of the acidic bridge hydroxyls of the zeolite with hydrocarbon molecules and the corresponding formation of H-bonds. Similar results are also given by Kotrel et al. [41] and by van Bokhoven et al. [42]. Under methanol flow (Fig. 10B), the band at 3477 cm^{-1} is not observed and the interaction between methanol and zeolite hydroxyls does not involve hydrogen bonding, since no new bands appeared in the v (OH) region [28–30]. This is due to the continuous flow conditions used. Furthermore, when the mixture stream of *n*-hexane and methanol is consecutively passed through the activated zeolite, a similar spectrum to that of methanol alone on the zeolite can be seen (Fig. 10C). These observations suggest that methanol is adsorbed on all acid sites prior to *n*-hexane when the co-reactants of *n*-hexane and methanol are fed to the zeolite.

3.4.2. Adsorption of methanol

Fig. 11 shows the difference spectra of methanol adsorption on HZSM-5 zeolite at different temperatures. Methanol adsorption is closely related to terminal silanol groups, AlOH groups, and the bridge hydroxyls of HZSM-5 zeolite, as seen from the negative features at 3744, 3667, and 3614 cm^{-1} [28–30]. The adsorption on bridge hydroxyl groups at 100 °C (Fig. 11a) gives the appearance of broad bands at 3560 and 3013 cm^{-1} (and at 2400–2500 and $1600–1700 \text{ cm}^{-1}$, not shown in Fig. 11a). These bands can be assigned to the OH

vibrations of the hydrogen-bonded methanol and of the methyl carboxonium ion ($CH_3OH_2^+$), formed by the attraction of the skeletal proton [29,30,43–45]. At the same time, some new bands could also be observed at 2971, 2954, and 2855 cm^{-1} (Fig. 11a–c). The band at 2855 cm^{-1} could be assigned to symmetric stretching vibrations of the CH_3 group of the adsorbed methanol, while the bands at 2954 and 2971 cm^{-1} could be due to asymmetric stretching vibrations of the CH_3 group of hydrogen-bonded methanol and $CH_3OH_2^+$, respectively [44,45]. As the temperature increases from 100 to 150 °C, the increase in the 2971 cm^{-1} band indicates that more methyl carboxonium ions are formed. In addition, two new bands appear at approximately 3300 and 2840 cm^{-1} at 150 °C due to the formation of DME [28,46], which is in good agreement with the TPSR results in Fig. 6.

At 200 °C, a new v (C–H) band appears at 2980 cm^{-1} as a poorly resolved shoulder on the high-frequency side of the 2971 cm^{-1} band in Fig. 11c. The 2980 cm^{-1} band increases accompanied by the appearance of a new band at 2867 cm^{-1} at temperatures higher than 250 °C (Fig. 11d–f). Both bands can be assigned to surface methoxy groups formed at Brønsted acid sites [28,30]. Surface methoxy groups were also successfully detected by solid-state ^{13}C MAS NUM spectroscopy for the methanol conversion on various solid acid catalysts [29,34]. According to Campo et al. [44] and Benito et al. [45], surface methoxy species can be formed through methanol or DME adsorption on the acidic site of the catalyst. The FT-IR results suggest that only a small fraction of $CH_3OH_2^+$ or $CH_3OHCH_3^+$ have been transferred into the methoxy groups at 200 °C, and that most adsorbed species
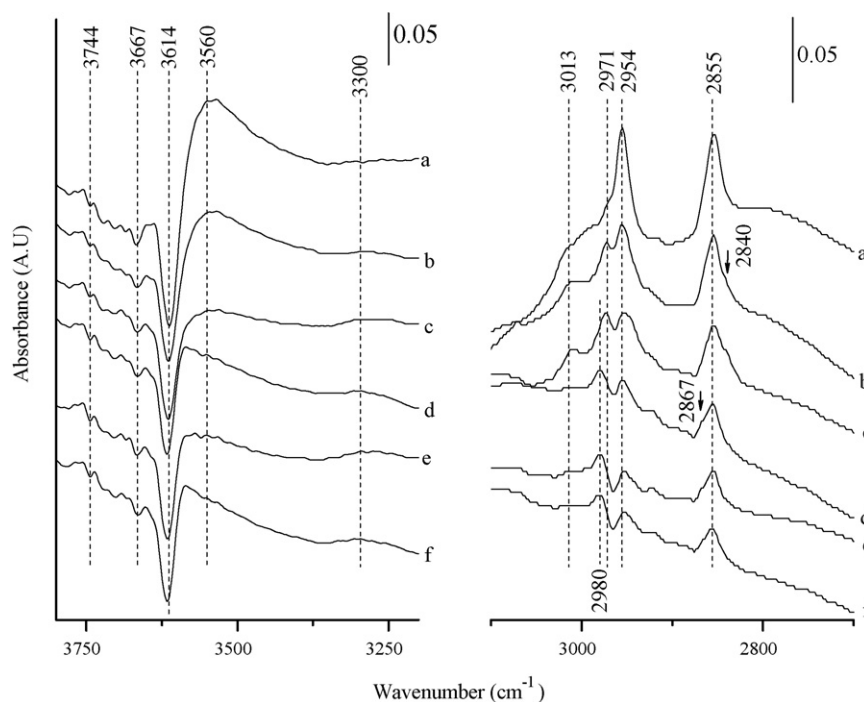
Fig. 11. Infrared difference spectra recorded after the adsorption of methanol on HZSM-5 zeolite at: (a) 100 °C; (b) 150 °C; (c) 200 °C; (d) 250 °C; (e) 300 °C; (f) 350 °C.

could transform into surface methoxy groups with temperature increase. These surface methoxy groups can still be detected at 350 °C.

4. Discussion

4.1. The effect of methanol on the conversion of n-hexane

The comparison of the coupled transformation of n-hexane and methanol with the conversion of n-hexane alone on HZSM-5 zeolite at 400 °C shows that the initial conversion of n-hexane is enhanced with methanol as co-reactant (Fig. 1). In the coupled reaction, methanol always shows a rather high conversion even at the shortest contact times employed (not shown in Fig. 1). The easy conversion property of methanol indicates that methanol molecules are first transformed into intermediate species on the acid sites, which is supported by the FT-IR results (Fig. 10). The band at 3477 cm^{-1}, due to hydrogen-bonding between n-hexane and hydroxyl groups of HZSM-5, could only be observed under n-hexane flow (Fig. 10A) and is absent in co-feed mixture flow and methanol flow (Fig. 10B and C). This may be caused by the proton affinity difference between n-hexane and methanol [47,48], which predicts that methanol is more strongly bonded by protonic sites. In this sense, the enhancement of the n-hexane activity can probably be attributed to the methanol transformation in the coupled system prior to the n-hexane adsorption and conversion, which means that the intermediate species or products from the methanol conversion are responsible for the improvement of the n-hexane activity.

4.2. The effect of intermediate species from methanol conversion on the transformation of n-hexane

TPSR measurements showed that the initial temperature of n-hexane cracking for n-hexane alone is much higher than that of the coupled reaction system (Fig. 4), suggesting that methanol could greatly improve the n-hexane activity on HZSM-5 zeolite catalyst. The temperature for the rapid consumption of methanol and DME is lowered to 310 °C for the coupled reaction (Fig. 6). However, the initial cracking temperature (220 °C) of n-hexane is much lower than the temperature at which methanol and DME are rapidly consumed. Therefore, the improvement of n-hexane activity might result from the intermediate species that arises from the conversion of methanol or DME below 310 °C. This improvement by the intermediate species was also proved by the catalytic tests over the catalyst with pre-adsorbed methanol between 200 and 350 °C (Fig. 9).

The infrared measurements of adsorbed methanol on the HZSM-5 zeolite catalyst suggest that the adsorbed species are surface methoxy groups when methanol contacts with the activated zeolite at 200–350 °C and that the chemisorbed methoxy groups exist up to 350 °C (Fig. 11). This is in good agreement with results reported by Wang et al. [31,34], who suggested that the active species are methoxy groups when methanol is passed through a zeolite catalyst bed at 200–250 °C. Kazansky and Senchenya suggested that surface methoxy groups are covalent in their ground state and more closely resemble the carbenium ion with partly positive charge when they act as the transition states at high reaction temperature [49]. Ono and Mori [35] also claimed that these

internal methoxy species are a kind of incipient methylcarbenium cation. The ionic character of methoxy groups at higher temperature was also emphasized by Hutchings et al. [50]. The enhancement of the *n*-hexane initial activity may thus stem from the participation of methoxy groups as active sites when methanol is used as co-reactant. In the present work, it seems more likely that the ionic methoxy groups attack *n*-hexane molecules more readily than the Brønsted acid sites on the zeolite surface.

Furthermore, we observed that the improvement of the *n*-hexane activity with pre-adsorbed methanol on the zeolite is different at different reaction temperatures. This temperature dependency might be attributed to two of the following factors: one is the change of ionic character of the methoxy groups and the other is the variation of amount of methoxy groups with temperature. The slight conversion increase at 200 °C could be due to the formation of a small quantity of methoxy groups with covalent character. With increasing temperature, most of the adsorbed methanol species transform into surface methoxy groups, as shown in Fig. 11. Their ionic character becomes more prominent according to the results given by Kazansky and Senchenya [49], meaning that their ability to activate *n*-hexane become stronger at high temperature than at low temperature. Further increasing temperature, desorption of methoxy groups and their interconversion would occur more readily. Therefore, the methanol-coupled *n*-hexane conversion is closely related to the surface methoxy species. All factors described above thus determine the most prominent coupling effect at 250 °C as shown in Fig. 9.

Fig. 3 shows that the initial formation rate of methane is different in the three reaction systems, suggesting that the mechanism of methane formation in the coupled system may be different from the other reaction systems. For the formation of methane from methanol, one possible explanation has been given by Fougerit et al. [51], who suggested that methane results from a direct hydride transfer between methoxy species and DME (or methanol) or/and from a secondary reaction. They also indicated that a demethylation of coke molecules would be possible. Tsoncheva and Dimitrova [52] and Schulz et al. [53] came to the same conclusion. In this work, the result is obtained by extrapolating to zero contact time, where methane formation from secondary reactions or demethylation of coke molecules should be negligible. Therefore, the initial formation of methane could be mainly from the interaction of methoxy groups and DME or methanol when the contact time tends to zero. For the reaction of *n*-hexane alone, methane appears just as the product of *n*-hexane monomolecular cracking. For the mixture of *n*-hexane and methanol as feed, the FT-IR results in Figs. 10 and 11 show that active sites are first occupied by methanol molecules and then transformed to surface methoxy groups. As a result, the monomolecular cracking of *n*-hexane is greatly suppressed due to the competitive adsorption of methanol, exhibiting the promotion effect of *n*-hexane conversion in the coupled system as confirmed by catalytic and TPSR results. This improvement may be from methoxy groups due to methanol adsorption and transformation. This

improvement may also be responsible for the highest initial formation rate of methane.

In Section 3.2.2, we noticed a different methane evolution with temperature in the three reaction systems. For methanol, the methane ($m/e = 16$) signal stays constant between 200 and 350 °C (Fig. 7b). This indicates that methane originates only from the interaction of methoxy groups and DME (or methanol). In the case of *n*-hexane alone (Fig. 7a), only trace amounts of methane are produced below 390 °C, meaning that no monomolecular *n*-hexane cracking occurs in this temperature range. However, when the mixture feed is used, the evolution of methane shows a maximum at 310 °C (Fig. 7c) instead of a constant value in the methanol transformation; no methane generation occurs in the *n*-hexane reaction. These observations predict that the methane production is improved with methanol coupling. It is therefore apparent that the rather high methane fraction detected in the coupled system must be attributed to the interactions between methoxy groups and *n*-hexane.

According to experimental studies [54–56] and theoretical calculations [49,57,58], there probably exist two ways of interaction between methoxy groups and *n*-hexane, viz. the protonation reaction and the hydride transfer. The two reactions are different in the formation of characteristic products [11,13]. Methane can be produced from both reactions, while the C_2 products and H_2 are only formed in the protonation reaction, and the evolutions of such H_2 and C_2 products are expected to show the similar tendency to that of methane. The TPSR results shown in Fig. 8 suggest that the evolutions of C_2 products and H_2 under the mixture flow did not exhibit a maximum as methane does. At the same time, it is worthy to note that the evolution profiles of $m/e = 2$ (H_2) and $m/e = 26$ (C_2 products) in the coupled system only exhibit the same tendency as those in the methanol alone system at low temperature, meaning that only methanol is responsible for the initial evolutions of H_2 and C_2 products in the coupled system. Thus, there appears to be no evidence from the TPSR results for the protonation reaction between *n*-hexane and methoxy groups to occur at low temperature. Therefore, the interaction of methoxy groups and *n*-hexane quite likely occurs through the hydride transfer reaction (Eq. (1)):

$$C_6H_{14} + CH_3-O-Z \rightarrow C_6H_{13}-O-Z + CH_4 \tag{1}$$
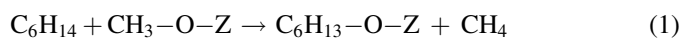
4.3. The effect of products from methanol conversion on the transformation of n-hexane

The catalytic results also show a change in the initial formation rates of the C_2–C_4 alkanes (Fig. 2). According to the alkane cracking and methanol conversion mechanisms, two routes can be envisaged for the initial formation of an alkane: direct formation by monomolecular cracking of *n*-hexane and bimolecular hydride transfer between alkane and alkene. Moreover, the apparent rate of the bimolecular mechanism is larger than that of the monomolecular mechanism [14,15,20,21]. In this work, the monomolecular cracking can only occur in the reaction of *n*-hexane alone. For the coupled

transformation, this route can be excluded because methanol will be adsorbed on all acid sites prior to n-hexane and immediately transformed into surface methoxy groups. In this case, two pathways can be considered for the reaction of methoxy groups: one pathway involving initial activation of n-hexane by the methoxy groups, and the other involving the interaction between methanol (or DME) and methoxy groups. As noted above, the latter is so fast that the alkene products, which are the major products of methanol conversion, may be quickly formed in the reaction system. These alkenes can further enhance the conversion of n-hexane via bimolecular H-transfer following the improvement by the methoxy groups. Therefore, it is clear that the abundant bimolecular H-transfer reactions between n-hexane and the C_3–C_4 alkenes, stemming from methanol transformation, result in faster formation rates of C_3–C_4 alkanes in the coupled reaction than in the individual reactant reaction. These observations suggest an additional contribution of alkene products from methanol conversion to the enhancement of n-hexane conversion after the improvement of methoxy groups. An exceptional case occurs in ethane formation, where the initial formation rate of ethane is the fastest in the n-hexane alone system. Considering the difficult formation of a primary ethylcarbenium ion from ethene [12,13,59], we can rule out the bimolecular pathway between ethene and n-hexane in the coupled system.

### 4.4. The effect of n-hexane on the conversion of methanol

The TPSR results shown in Fig. 6 suggest that the equilibration among methanol, DME, and water in the methanol-alone system will be maintained up to 350 °C. Beyond this temperature, the methanol and DME profiles show sharp decreases in intensity. Moreover, this temperature region coincides with the appearance of a second water peak and aliphatic hydrocarbons. This is in good agreement with results reported by some authors [35,51,60,61]. According to these authors, the conversion of methanol is an autocatalytic process with an induction period. As soon as the first C–C band is

formed, the rate of methanol consumption is rapidly accelerated. Compared with the conversion of methanol alone, the temperature at which methanol and DME are rapidly consumed starts at 310 °C in the coupled system, which suggests an acceleration of methanol conversion by the species from the conversion of n-hexane. Considering the mechanism of methanol conversion, some authors suggested the "hydrocarbon pool" mechanism [24–27], with an induction period needed for pool formation. In the present study, participation of methanol into the n-hexane conversion and the interaction between two reactants leads the methanol conversion to occur in other possible ways parallel to the C–C bond assembly with the aid of hydrocarbon pool. This multi-route conversion could be used to explain the acceleration of methanol conversion in the coupled system. Further studies on the detailed mechanisms for the acceleration of methanol conversion in the coupled system will be reported in our next study.

4.5. Proposed reaction pathway of n-hexane activation with methanol as co-reactant

The improved conversion of n-hexane (Sections 3.1–3.3) predicts that activation and transformation of n-hexane occurs in a particular way in the coupled reaction system. The FT-IR results (Section 3.4) had provided information on the competitive adsorption of n-hexane and methanol. The strong methanol adsorption, accompanied by the character of intermediate species and product generation, allow us to propose the following reaction mechanism to correlate all observations.

The conversion of n-hexane in the coupled reaction comprises an initial step in which the hydride transfer reaction starts with an attack of n-hexane by the surface methoxy groups from methanol transformation. As shown in Scheme 1a, this attack results in stretching and strong polarization of the C–O bond and formation of the adsorbed nonclassical $[C_6H_{13}$–H–$CH_3]^+$ carbonium ion. Decomposition of this activated complex results in elimination of a methane molecule and
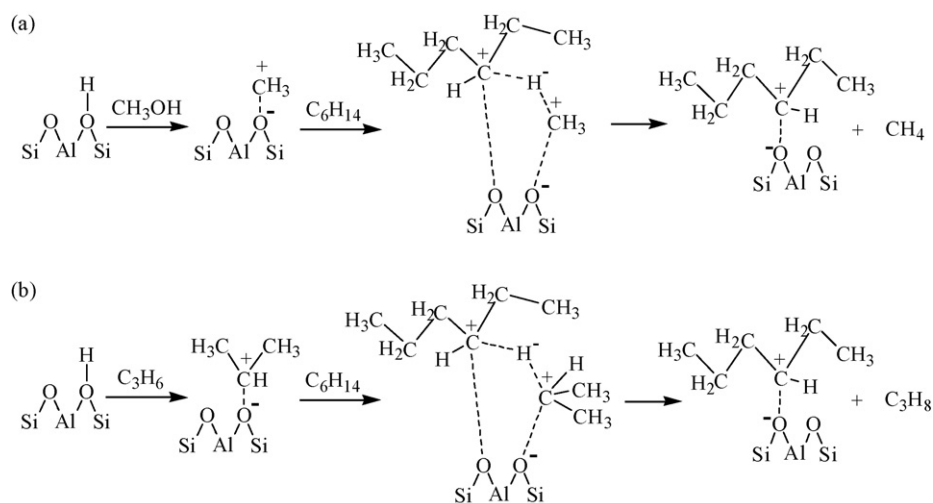
Scheme 1. An adsorbed methoxy species (a) and an adsorbed propoxy species (b) derived from methanol activating the feed n-hexane molecule through the bimolecular H-transfer route.

formation of the corresponding carbenium ion $[C_6H_{13}]^+$. At the same time, the acceleration of methanol conversion due to the *n*-hexane activation would lead to the fast formation of alkene products. These alkenes will further enhance the conversion of *n*-hexane via bimolecular hydride transfer reaction, which may be an important step responsible for chain propagation of *n*-hexane conversion in the coupled system. As an example, the hydride transfer reaction between propene and *n*-hexane is described in Scheme 1b, which results in the formation of a propane molecule and the corresponding carbenium ion $[C_6H_{13}]^+$.

5. Conclusions

Coupling of the conversion of *n*-hexane and methanol brought a great improvement of the *n*-hexane transformation. A high initial conversion rate and low starting reaction temperature of *n*-hexane were proved by the pulse catalytic tests and TPSR measurements. Methoxy groups, as the most important intermediate, absent in the transformation of pure *n*-hexane and generated by methanol adsorption and conversion over the zeolite surface, were found with FT-IR. In the temperature range of 200–350 °C, a predominant coupling effect could be observed. This temperature dependence corresponded to the generation and evolution of methoxy groups with temperature. Methane appeared as characteristic product in the coupling reaction system. In addition, the initial formation rates of propane and butane improved with methanol incorporation into the reaction.

A mechanism is proposed to explain the possible reaction route of this coupling reaction system. The intermediate species and products from the methanol conversion worked as the active sites for the *n*-hexane conversion. They are responsible for the initial activation and chain propagation of *n*-hexane via bimolecular hydride transfer. These proposed reaction routes also explain the acceleration of the methanol conversion in the coupled system.

References

[1] Y.X. Wei, Z.M. Liu, G.W. Wang, Y. Qi, L. Xu, P. Xie, Y.L. He, Stud. Surf. Sci. Catal. 158 (2005) 1223–1230.
[2] Y. Yoshimura, K. Matano, F. Mizukami, Shokubai, Stud. Surf. Sci. Catal. 43 (3) (2001) 218–223.
[3] C.D. Chang, A.J. Silvestri, J. Catal. 47 (1977) 249–259.
[4] C.D. Chang, Catal. Rev. Sci. Eng. 25 (1983) 1–118.
[5] S. Nowak, H. Günschel, A. Martin, K. Anders, B. Lücke, in: Proceedings of the 9th International Congress on Catalysis, vol. 4, Chem. Inst. Can., Ottawa, Ont., 1988, pp. 1735–1742.
[6] B. Lücke, A. Martin, Micropor. Mesopor. Mater. 29 (1999) 145–157.
[7] Z.X. Gao, R.C. Cheng, Y.C. Tan, Q.H. Zhu, J. Fuel. Chem. Technol. 23 (4) (1995) 349–354.
[8] V.L. Erofeev, L.B. Shabalina, L.M. Koval, T.S. Minakova, Russ. J. Appl. Chem. 75 (12) (2002) 752–754.
[9] M. Stöcker, Micropor. Mesopor. Mater. 29 (1999) 3–48.
[10] J.F. Haw, W.G. Song, D.M. Marcus, J.B. Nicholas, Acc. Chem. Res. 36 (2003) 317–326.
[11] A. Corma, A.V. Orchillés, Micropor. Mesopor. Mater. 35/36 (2000) 21–30.
[12] V.Y. Kissin, Catal. Rev. Sci. Eng. 43 (1/2) (2001) 85–147.
[13] F.C. Jentoft, B.C. Gates, Topics Catal. 4 (1997) 1–13.
[14] W.O. Haag, R.M. Dessau, R.M. Lago, Stud. Surf. Sci. Catal. 60 (1991) 255–265.
[15] W.O. Haag, R.M. Dessau, in: Proceedings of the 8th International Congress on Catalysis, vol. 2, Verlag Chemie, Weinheim, 1994, pp. 305–316.
[16] P.V. Shertuked, G. Marcelin, G.A. Sill, W.K. Hall, J. Catal. 136 (1992) 446–462.
[17] A.F.H. Wielers, M. Vaarkamp, M.F.M. Post, J. Catal. 127 (1991) 51–66.
[18] S. Jolly, J. Saussey, M.M. Bettahar, J.C. Lavalley, E. Benazzi, Appl. Catal. A 156 (1997) 71–96.
[19] S.M. Babitz, B.A. Williams, J.T. Miller, R.Q. Snurr, W.O. Haag, H.H. Kung, Appl. Catal. A 179 (1999) 71–86.
[20] B.A. Williams, W. Ji, J.T. Miller, R.Q. Snurr, H.H. Kung, Appl. Catal. A 203 (2000) 179–190.
[21] B.A. Williams, J.T. Miller, R.Q. Snurr, H.H. Kung, Micropor. Mesopor. Mater. 35/36 (2000) 61–74.
[22] J. Abbot, J. Catal. 123 (1990) 383–395.
[23] D.M. Anufriev, P.N. Kuznetsov, K.G. Ione, J. Catal. 65 (1980) 221–226.
[24] I.M. Dahl, S. Kolboe, J. Catal. 149 (1994) 458–464.
[25] B. Arsted, S. Kolboe, J. Am. Chem. Soc. 123 (2001) 8137–8138.
[26] M. Seiler, W. Wang, A. Buchholz, M. Hunger, Catal. Lett. 88 (3/4) (2003) 187–191.
[27] P.W. Goguen, T. Xu, D.H. Barich, T.W. Skloss, W.G. Song, Z.K. Wang, J.B. Nicholas, J.F. Haw, J. Am. Chem. Soc. 120 (1998) 2650–2651.
[28] T.R. Forester, R.F. Howe, J. Am. Chem. Soc. 109 (1987) 5076–5082.
[29] S.M. Campbell, X.Z. Jiang, R.F. Howe, Micropor. Mesopor. Mater. 29 (1999) 91–108.
[30] L. Kubelková, J. Nováková, K. Nedomová, J. Catal. 124 (1990) 441–450.
[31] W. Wang, M. Seiler, M. Hunger, J. Phys. Chem. B 105 (2001) 12553–12558.
[32] C.M.Z. Wilson, P. Viruela, A. Corma, J. Phys. Chem. 99 (1995) 13224–13231.
[33] S.R. Blaszkowski, R.A. van Santen, J. Phys. Chem. B. 101 (1997) 2292–2305.
[34] W. Wang, A. Buchholz, M. Seiler, M. Hunger, J. Am. Chem. Soc. 125 (2003) 15260–15267.
[35] B.Y. Ono, T. Mori, J. Chem. Soc. Faraday. Trans. 77 (1981) 2209–2221.
[36] F. Haase, J. Sauer, J. Am. Chem. Soc. 117 (1995) 3780–3789.
[37] F.X. Chang, Y.X. Wei, X.B. Liu, Y. Qi, D.Z. Zhang, Y.L. He, Z.M. Liu, Catal. Lett. 106 (2006) 171–176.
[38] NIST, 98. Database.
[39] J. Rakoczy, T. Romotowski, Zeolites 13 (1993) 256–260.
[40] M. Trombetta, T. Armaroli, A.G. Alejandre, J.R. Solis, G. Busca, Appl. Catal. A 192 (2000) 125–136.
[41] S. Kotrel, M.P. Rosynek, J.H. Lunsford, J. Catal. 191 (2000) 55–61.
[42] J.A. van Bokhoven, M. Tromp, D.C. Koningsberger, J.T. Miller, J.A.Z. Pieterse, J.A. Lercher, B.A. Williams, H.H. Kung, J. Catal. 202 (2001) 129–140.
[43] S.R. Blaszkowski, R.A. van Santen, Stud. Surf. Sci. Catal. 105 (1997) 1707–1714.
[44] A.E.S. Campo, A.G. Gayubo, A.T. Aguayo, A. Tarrío, J. Bilbao, Ing. Eng. Chem. Res. 37 (1998) 2336–2340.
[45] P.L. Benito, A.G. Gayubo, A.T. Aguayo, M. Olazar, J. Bilbao, J. Chem. Technol. Biotechnol. 66 (1996) 183–191.
[46] P. Tynjälä, T.T. Pakkanen, S. Mustamäki, J. Phys. Chem. B 102 (1998) 5280–5286.
[47] B. Sowerby, S.J. Becker, L.J. Belcher, J. Catal. 161 (1996) 377–386.
[48] J.F. Haw, Phys. Chem. Chem. Phys. 4 (2002) 5431–5441.
[49] V.B. Kazansky, I.N. Senchenya, J. Catal. 119 (1989) 108–120.
[50] G.J. Hutchings, G.W. Watson, D.J. Willock, Micropor. Mesopor. Mater. 29 (1999) 67–77.
[51] J.M. Fougerit, N.S. Gnep, M. Guisnet, Micropor. Mesopor. Mater. 29 (1999) 79–89.
[52] T. Tsoncheva, R. Dimitrova, Appl. Catal. A 225 (2002) 101–107.
[53] H. Schulz, D. Barth, Z. Siwei, Stud. Surf. Sci. Catal. 68 (1991) 783–790.
[54] R.P. Clow, J.H. Futrell, J. Am. Chem. Soc. 94 (1972) 3748–3755.
[55] R. Houriet, G. Parisod, T. Gäumann, J. Am. Chem. Soc. 99 (1977) 3599–3602.

[56] S. Mark, C. Schellhammer, G. Niedner-Schatteburg, D. Gerlich, J. Phys. Chem. 99 (1995) 15587–15594.

[57] V.B. Kazansky, M.V. Frash, Catal. Lett. 28 (1994) 211–222.

[58] V.B. Kazansky, M.V. Frash, R.A. van Santen, Catal. Lett. 48 (1997) 61–67.

[59] B.G. Anderson, R.R. Schumacher, R. van Duren, A.P. Singh, R.A. van Santen, J. Mol. Catal. A 181 (2002) 291–301.

[60] E. Lglesia, T. Wang, S.Y. Yu, Stud. Surf. Sci. Catal. 119 (1998) 527–532.

[61] M. Jayamurthy, S. Vasudevan, Catal. Lett. 36 (1996) 111–114.